

# Pressure isotropization in high energy heavy ion collisions

Thomas Epelbaum\* and François Gelis†

*Institut de Physique Théorique, CEA/Saclay, 91191 Gif sur Yvette cedex, France*

(Dated: February 25, 2022)

The early stages of high energy heavy ion collisions are studied in the Color Glass Condensate framework, with a real-time classical lattice simulation. When increasing the coupling constant, we observe a rapid increase of the ratio of longitudinal to transverse pressure. The transient regime that precedes this behavior is of the order of 1 fm/c.

## INTRODUCTION

Heavy ion collisions at ultrarelativistic energies are currently being performed at the Relativistic Heavy Ion Collider (RHIC) and the Large Hadron Collider (LHC), in order to study the properties of nuclear matter at extreme temperatures and densities. Models that assume that the fireball produced in these collisions expands according to the laws of relativistic hydrodynamics have been very successful in reproducing the behavior of many bulk observables [1–4].

Hydrodynamical flow follows from energy-momentum conservation, but also assumes that the energy-momentum tensor of the system is sufficiently close to that of a perfect fluid, that reads

$$T_{\text{perfect}}^{\mu\nu} = \text{diag}(\epsilon, p, p, p), \quad (1)$$

where  $\epsilon$  is the energy density and  $p$  the pressure (related to  $\epsilon$  by an equation of state). In particular, the pressure tensor of a perfect fluid at rest is isotropic. A limited amount of pressure anisotropy can be accommodated in the hydrodynamical description by adding to eq. (1) some viscous corrections.

Understanding why the pressure tensor becomes nearly isotropic in terms of the underlying Quantum-Chromodynamics (QCD) dynamics has so far been very challenging [5]. At high energy, the density of constituents (mostly gluons) in the two nuclei is large, and a consistent QCD description can be achieved in the Color Glass Condensate (CGC) framework [6, 7]. The CGC is designed to collect and sum all the recombination and multiple scattering corrections that are prevalent at high gluon density. These nonlinear effects are controlled by a unique dimensionful parameter, the saturation momentum  $Q_s$ , that increases with energy.

For inclusive quantities, like the expectation value of the energy-momentum tensor, the CGC provides an expansion in powers of the strong coupling constant  $\alpha_s = \frac{g^2}{4\pi}$ , in which the leading order (LO) is obtained by solving the classical Yang-Mills equations. Immediately after the collision (proper time  $\tau = 0^+$ , see the figure 1), the CGC gives the following energy-momentum tensor at LO [8],

$$T_{\text{CGC,LO}}^{\mu\nu} = \text{diag}(\epsilon, \epsilon, \epsilon, -\epsilon). \quad (2)$$

The longitudinal pressure is negative, exactly opposite to the energy density and the transverse pressure, and therefore quite far from the near ideal form expected when hydrodynamics is applicable.

However, for anisotropic systems, classical solutions of the Yang-Mills equations are subject to Weibel instabilities that make them exponentially sensitive to their initial conditions [9, 10]. These instabilities are triggered by next-to-leading order (NLO) corrections, in which they cause secular divergences, i.e. terms that are of higher order in the coupling  $\alpha_s$  but accompanied by a coefficient that becomes infinite when  $\tau \rightarrow +\infty$ . These secular terms break the simple power counting that organizes the expansion in power of  $\alpha_s$ . It is however possible to resum at all orders in  $\alpha_s$  the terms that grow the fastest in time [11, 12], by allowing the initial fields to fluctuate with a Gaussian distribution whose variance is given by a 1-loop calculation.

This resummed result includes the LO and NLO contributions, plus a subset of all the higher orders, and it remains finite at all times. Moreover, it has been shown in the case of a scalar theory that this reorganization of the perturbative expansion leads to the near isotropy of the pressure tensor, and to a good agreement with nearly ideal hydrodynamics [13]. The purpose of this paper is to study this resummation in the case of Yang-Mills theory, which is directly relevant for heavy ion collisions. We use the classical statistical approach –performing a Monte-Carlo sampling of the Gaussian ensemble of classical initial conditions and solving numerically the classical Yang-Mills equations in real time on a 3 dimensional lattice– in order to study the time dependence of the energy-momentum tensor shortly after the collision.

## SPECTRUM OF INITIAL CONDITIONS

In the absence of quantum fluctuations (i.e. at LO), the initial gauge fields and electrical fields are given by classical solutions of the Yang-Mills equations in the presence of two light-cone color currents representing the two

nuclei. At  $\tau = 0^+$ , these solutions read

$$\begin{aligned} A_0^i &= \alpha_1^i + \alpha_2^i, \quad E_0^i = 0, \quad \alpha_n^i = \frac{i}{g} U_n^\dagger \partial^i U_n, \\ A_{0\eta} &= 0, \quad E_0^\eta = i \frac{g}{2} [\alpha_1^i, \alpha_2^i], \end{aligned} \quad (3)$$

where the Wilson lines  $U_{1,2}(\mathbf{x}_\perp)$  read

$$U_1(\mathbf{x}_\perp) = \text{T} e^{ig \int dx^- \frac{1}{\nabla_\perp^2} \rho_1(x^-, \mathbf{x}_\perp)} \quad (4)$$

in the McLerran-Venugopalan model [14]. The saturation momentum  $Q_s$  controls the event-by-event fluctuations of the color charge density  $\rho_1$

$$g^2 \int dx^- dy^- \langle \rho_1^a(x) \rho_1^b(y) \rangle = \delta^{ab} Q_s^2 \delta(\mathbf{x}_\perp - \mathbf{y}_\perp). \quad (5)$$

The  $U_2$  of the second nucleus is obtained similarly. To this background field, we add a fluctuating component, to obtain

$$\begin{aligned} A^\mu(x) &= A_0^\mu(x) + \sum_{c,\lambda} \int \frac{d^3 \mathbf{k}}{(2\pi)^3 2k} \left[ c_{c\lambda \mathbf{k}} a_{c\lambda \mathbf{k}}^\mu(x) + \text{c.c.} \right] \\ E^\mu(x) &= E_0^\mu(x) + \sum_{c,\lambda} \int \frac{d^3 \mathbf{k}}{(2\pi)^3 2k} \left[ c_{c\lambda \mathbf{k}} e_{c\lambda \mathbf{k}}^\mu(x) + \text{c.c.} \right] \end{aligned} \quad (6)$$

where  $a_{c\lambda \mathbf{k}}^\mu(x)$  ( $e_{c\lambda \mathbf{k}}^\mu(x)$  is the conjugate electrical field) is the solution of the linearized Yang-Mills equations over the background field  $A_0^\mu$ , with as initial condition at  $x^0 = -\infty$  a plane wave of color  $c$ , polarization  $\lambda$  and momentum  $\mathbf{k}$ . The coefficients  $c_{c\lambda \mathbf{k}}$  are complex Gaussian distributed random numbers, whose variance is

$$\langle c_{c\lambda \mathbf{k}} c_{c'\lambda' \mathbf{k}'}^* \rangle = (2\pi)^3 k \delta_{cc'} \delta_{\lambda\lambda'} \delta(\mathbf{k} - \mathbf{k}'). \quad (7)$$

Note that the background field is of order  $Q_s/g$  while the fluctuating part is of order  $Q_s$ .

The mode functions  $a_{c\lambda \mathbf{k}}^\mu(x)$ ,  $e_{c\lambda \mathbf{k}}^\mu(x)$  have been determined analytically in Ref. [15] (see the Eqs. (69) in this reference), in terms of formulas involving only Fourier integrals, at a time  $\tau_0 \ll Q_s^{-1}$  (i.e. just after the collision). Numerically, we proceed as follows:

- i. Compute the background fields according to Eqs. (3). Since we are interested in studying isotropization in a given event, a single configuration of this background field is generated.
- ii. Generate random Gaussian numbers  $c_{c\lambda \mathbf{k}}$ , and evaluate Eqs. (6) at some small initial time  $\tau_0 \ll Q_s^{-1}$ ,
- iii. Using this configuration  $A^\mu, E^\mu$  as initial condition at  $\tau_0$ , solve the classical Yang-Mills equations  $\partial_0 A^\mu = E^\mu$ ,  $\partial_0 E^\mu = D_i F^{i\mu} + D_\eta F^{\eta\mu}$  (written here in temporal gauge  $A^0 = 0$ ) up to the largest time of interest,
- iv. Evaluate the observable in terms of this classical solution,
- v. Repeat the steps ii–iv in order to sample the ensemble of fluctuating initial conditions.

## SIMULATION SETUP

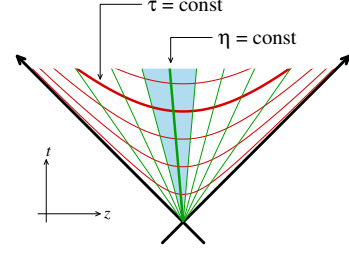


FIG. 1. Comoving coordinate system in the forward light-cone of the collision point.

In order to cope with the longitudinal expansion of the system, we use the comoving coordinates  $\tau \equiv \sqrt{t^2 - z^2}$  (proper time) and  $\eta \equiv \frac{1}{2} \ln(t+z)/(t-z)$  (rapidity). As illustrated in the figure 1, a constant extent in rapidity corresponds to a volume that expands in the longitudinal direction as time increases.

We solve the Yang-Mills equations numerically by discretizing space, while time remains a continuous variable whose increments can be arbitrarily small, as needed to ensure the accuracy of the solution. Due to limited computational resources, we do not simulate the entire interaction zone, but only a smaller sub-volume, both in the transverse directions and in rapidity (see the figure 2). For reasons related to the longitudinal expansion of the

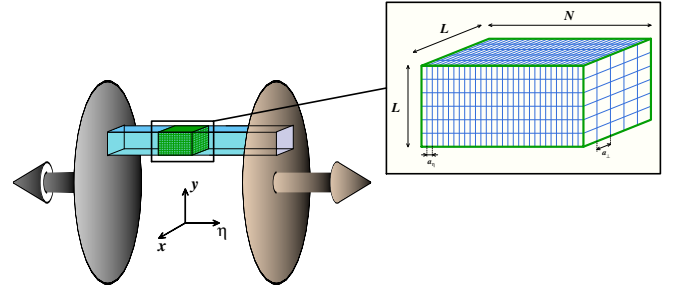


FIG. 2. Lattice setup.

system, it is necessary to have a larger number ( $N$ ) of lattice intervals in the longitudinal direction than in the transverse ones ( $L$ ).

The results presented in this paper were obtained on a  $64 \times 64 \times 128$  lattice with  $N_{\text{conf}}$  field configurations in the Monte-Carlo sampling. The lattice spacing in the rapidity direction is set to  $a_\eta = 1/64$ , so that our lattice covers two units of rapidity. The saturation momentum  $Q_s$  was chosen such that  $Q_s a_\perp = 1$ , i.e. significantly below the lattice ultraviolet cutoff for transverse momenta ( $k_\perp^{\text{max}} a_\perp = \sqrt{8}$ ). A study of the dependence on the lattice parameters, that may affect our results, will be performed in a future work. The field configurations are generated at the initial time  $Q_s \tau_0 = 0.01$ , but the sub-

sequent results do not depend on this choice as long as  $Q_s \tau_0 \ll 1$ . In order to simplify the color algebra, the simulation is done for an SU(2) gauge group, instead of SU(3) for actual QCD.

We work in Fock-Schwinger gauge,  $A^\tau = 0$ , that generalizes the temporal gauge to the  $(\tau, \eta, \mathbf{x}_\perp)$  system of coordinates, and has the advantage of treating the two nuclei on the same footing. On the lattice, the vector potentials are exponentiated into link variables that connect adjacent lattice sites in order to preserve an exact local gauge symmetry. However, exponentiating the vector potentials in Eqs. (6) introduces some small violations of Gauss's law  $D_\mu E^\mu = 0$ . We restore Gauss's law by projecting the initial electrical fields on the subspace that obeys the constraint, using the algorithm described in Ref. [16].

## ENERGY-MOMENTUM TENSOR

From the solutions of the classical Yang-Mills equations at some time  $\tau$ , we compute the expectation value of the components of the energy momentum tensor. In order to increase the effective statistics, we average both over the random numbers  $c_{\nu\lambda\mathbf{k}}$  of Eqs. (6) and over the lattice volume. At all times, the transverse and longitudinal pressures are related to the energy density by  $\epsilon = 2P_T + P_L$  (by construction), and Bjorken's law,

$$\frac{\partial \epsilon}{\partial \tau} + \frac{\epsilon + P_L}{\tau} = 0, \quad (8)$$

is satisfied as a consequence of energy and momentum conservation.

The energy-momentum tensor computed in this approach contains a zero point contribution, that exists even when the background field in Eqs. (3) is set to zero. We subtract it out by performing the same calculation twice: with a background field generated with a non-zero value of  $Q_s$  and with the background field set to zero.

After this pure vacuum subtraction,  $\epsilon$  and  $P_L$  still contain subleading divergences that behave as  $\tau^{-2}$ . Although we cannot compute the corresponding counterterms from first principles at the moment, their form can be predicted. From  $\epsilon = 2P_T + P_L$ , the counterterms for  $\epsilon$  and  $P_L$  must be equal. Then Bjorken's law (8) constrains this common counterterm to be of the form  $A/\tau^2$ . We fit the prefactor  $A$  in order to make  $\epsilon$  and  $P_L$  finite in the limit  $\tau \rightarrow 0^+$ . This choice of  $A$  also makes the resummed and Leading Order results very close when  $\tau \rightarrow 0^+$ , which is expected since the higher order corrections should be important only at later times, after the fluctuations have been amplified by the Weibel instability.

To summarize our procedure, we do

$$\begin{aligned} \langle P_T \rangle_{\text{phys.}} &= \langle P_T \rangle_{\text{backgd.} + \text{fluct.}} - \langle P_T \rangle_{\text{fluct. only}} \\ \langle \epsilon, P_L \rangle_{\text{phys.}} &= \underbrace{\langle \epsilon, P_L \rangle_{\text{backgd.} + \text{fluct.}}}_{\text{computed}} - \underbrace{\langle \epsilon, P_L \rangle_{\text{fluct. only}}}_{\text{computed}} + \underbrace{A \tau^{-2}}_{\text{fitted}}. \end{aligned} \quad (9)$$

It should be noted that the zero point contribution also behaves as  $\tau^{-2}$  at small times and is almost independent of the coupling, while the physical contribution is of order  $Q_s^4/g^2$ . At large coupling and small times, the physical contribution is much smaller than the two terms that we must subtract, and therefore the accuracy on the difference is severely limited by the statistical errors. This limits how large the coupling constant  $g$  can be in practical simulations. The results presented below are for  $g = 0.1$  (figure 3,  $N_{\text{conf}} = 200$ ) and  $g = 0.5$  (figure 4,  $N_{\text{conf}} = 2000$ ), that are both much smaller than the expected value at the LHC ( $g \approx 2$ ).

To provide more intuition on the relevant timescales, we also provide the time in fermis/c on the upper horizontal scale of the figures 3 and 4. The calibration of this scale requires that one chooses the value of  $Q_s$  in GeV, here taken to be  $Q_s = 2$  GeV, a reasonable value for nucleus-nucleus collisions at LHC energies. In order to highlight the effect of the quantum corrections, we also show the Leading Order results (dotted curves).

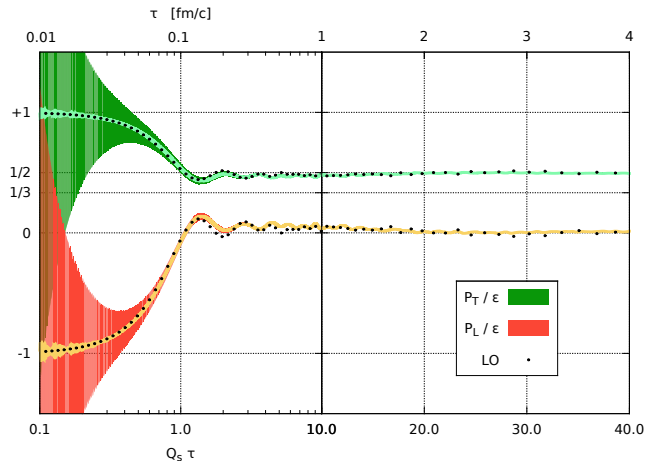


FIG. 3. Evolution of the ratios  $P_{T,L}/\epsilon$  for  $g = 0.1$  ( $\alpha_s = 8 \cdot 10^{-4}$ ). The bands indicate statistical errors, estimated as the result obtained before any subtraction divided by the square root of the number of samples. The dotted curves represent the LO result.

In both cases,  $\epsilon = P_T = -P_L$  at  $\tau = 0^+$ . After a time of order  $Q_s^{-1}$ , the longitudinal pressure turns positive and stays mostly positive afterwards. However, for  $g = 0.1$  it always stays much smaller than the transverse pressure ( $P_L/P_T \approx 0.01$ ), which implies that the system is almost free streaming in the longitudinal direction: the energy

density decreases approximately as  $\tau^{-1}$ . Moreover, the result are always very close to the LO results, suggesting that at such small couplings the Weibel instability does not play an important role over the timescales we have considered.

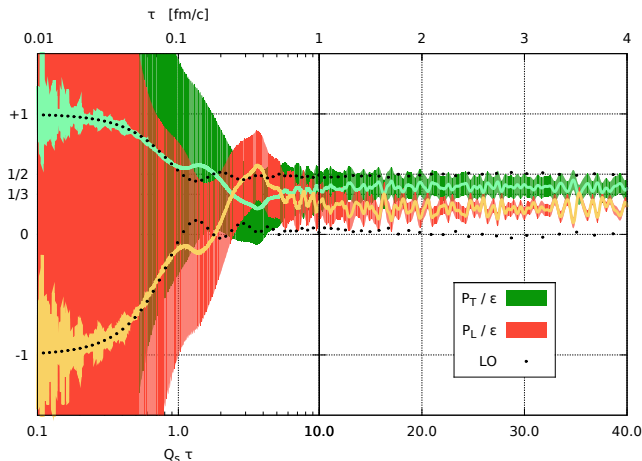


FIG. 4. Evolution of the ratios  $P_{T,L}/\epsilon$  for  $g = 0.5$  ( $\alpha_s = 2 \cdot 10^{-2}$ ).

Even though  $g = 0.5$  is still a very weak coupling in QCD, there is drastic increase in the ratio  $P_L/P_T$ , that now approaches 0.60 at times of the order of one fm/c. As a consequence,  $\epsilon$  falls faster than in free streaming because of the energy reduction due to the work done by the longitudinal pressure. Such a degree of residual anisotropy can easily be coped with in hydrodynamics with moderate viscous corrections. Note that the pressures have some residual oscillations on shorter timescales of order  $Q_s^{-1}$ , that do not affect the long time dynamics. The comparison with the LO result now indicates sizable deviations when  $Q_s \tau \gtrsim 1$ . Note that the LO results are identical for  $g = 0.1$  and  $g = 0.5$ , since at this order the energy-momentum tensor is given by purely classical field configurations, from which the coupling dependence can be entirely factored out.

We have also fitted the time dependence of  $\epsilon$  for  $g = 0.5$  by assuming that it is governed by hydrodynamics including the first correction due to shear viscosity,  $\epsilon = a/\tau^{4/3} - 2\eta_0/\tau^2$ . This gives an estimate of the shear viscosity  $\eta = \eta_0/\tau$  from which we obtain the dimensionless ratio  $\eta/\epsilon^{3/4} \approx \eta_0/a^{3/4} \approx 0.3$ , which is much smaller than the LO perturbation theory value, of order  $\sim 300$  for  $g = 0.5$  (see Ref. [17] for  $\eta$ . For  $\epsilon$ , we use the Stefan-Boltzmann formula). This is possibly a manifestation of the anomalously small viscosity conjectured in Ref. [18] for systems made of strong disordered fields.

Although the figure 4, that exhibits isotropization, was obtained for a coupling which is still much smaller than the  $\alpha_s \approx 0.3$  (i.e.  $g \approx 2$ ) that is expected at the LHC, we do not expect important qualitative modifications by

going at larger coupling. Moreover, the timescales should not vary much either (and if anything, one would expect them to become smaller) since the  $g$  dependence is to a large extent cancelled by the fact that the background fields behave as  $g^{-1}$ .

## CONCLUSIONS AND OUTLOOK

In this paper, we have presented the first NLO-resummed results in the Color Glass Condensate framework for the energy-momentum tensor shortly after a heavy ion collision. At very small coupling, the system settles on a free-streaming expansion curve, which is not compatible with ideal hydrodynamics.

However, by increasing the coupling constant, one reaches a regime of viscous hydrodynamical expansion, after a fairly short transient regime that lasts about 1 fm/c for realistic values of the saturation momentum. This hydrodynamical regime sets in for very small values of the coupling constant ( $g = 0.5, \alpha_s = 2 \cdot 10^{-2}$  in the plots presented above). Although it was not technically feasible to have a more realistic value of  $g$ , we conjecture a similar behavior at larger  $g$ . Conversely, the experimental evidence for hydrodynamical flow in heavy ion collisions does not necessarily imply that the system is strongly coupled, since weak coupling techniques and resummations already predict such a behavior.

More systematic studies are necessary in order to assess how one goes from free streaming at very weak coupling to hydrodynamical behavior for larger couplings. Moreover, the present study does not tell how far the system is from local thermal equilibrium when the hydrodynamical behavior starts. It would be highly interesting to compute observables that can provide informations on this question. Recent works, such as Refs. [19–24], have investigated the possibility of the formation of Bose-Einstein condensate when starting from a CGC-like initial condition, since such a state is overpopulated. It would definitely be important to assess this question in the present framework. Another important issue is to develop a rigorous procedure for the subtractions that we have performed by hand in order to obtain a finite energy-momentum tensor at short times. Moreover, higher order quantum corrections not included here are expected to become important at late times. Including them is beyond the scope of classical statistical methods, but at the small couplings we have considered we do not expect them to be important at the times relevant for pressure isotropization.

This study is related to other recent works on the effect of instabilities on the early time behavior in heavy ion collisions, in particular Refs. [25–30]. The approach we have pursued, where one solves the classical Yang-Mills equations with fluctuating initial conditions, is very close to that of Ref. [30], but differs from it in the choice of the

ensemble of initial fields. In the present work, we have used the analytical solutions (derived in Ref. [15]) for the mode functions over the CGC classical gauge fields produced in heavy ion collisions, while Ref. [30] used vacuum mode functions, rescaled in order to obtain a prescribed occupation number at a larger initial time of order  $\tau_0 \approx 100 Q_s^{-1}$ . In the future, it would be interesting to see whether the CGC initial conditions (that have small fluctuations around a large coherent field) used in the present paper eventually evolve into the ensemble of fields (that have no coherent field and large fluctuations) used as the starting point in Ref. [30].

### ACKNOWLEDGEMENTS

We thank J. Berges, W. Broniowski, J.-P. Blaizot, L. McLerran, J.-Y. Ollitrault, S. Schlichting, R. Venugopalan and B. Wu for discussions related to this work. This work is supported by the Agence Nationale de la Recherche project 11-BS04-015-01. Some of the computations were performed with the resources provided by GENCI-CCRT (project t2013056929).

---

\* thomas.epelbaum@cea.fr

† francois.gelis@cea.fr

- [1] D. Teaney, Prog. Part. Nucl. Phys. **62**, 451 (2009).
- [2] D. Teaney, arXiv:0905.2433.
- [3] J.Y. Ollitrault, J. Phys. Conf. Ser. **312**, 012002 (2011).
- [4] J.Y. Ollitrault, F. Gardim, Nucl. Phys. **A 904–905**, 75c (2013).
- [5] J. Berges, J.P. Blaizot, F. Gelis, J. Phys. **G 39**, 085115 (2012).

- [6] T. Lappi, Int. J. Mod. Phys. **E20**, 1 (2011).
- [7] F. Gelis, E. Iancu, J. Jalilian-Marian, R. Venugopalan, Ann. Rev. Part. Nucl. Sci. **60**, 463 (2010).
- [8] T. Lappi, L.D. McLerran, Nucl. Phys. **A 772**, 200 (2006).
- [9] P. Romatschke, R. Venugopalan, Phys. Rev. Lett. **96**, 062302 (2006).
- [10] P. Romatschke, R. Venugopalan, Phys. Rev. **D 74**, 045011 (2006).
- [11] F. Gelis, T. Lappi, R. Venugopalan, Phys. Rev. **D 78**, 054019 (2008).
- [12] K. Dusling, F. Gelis, R. Venugopalan, Nucl. Phys. **A 872**, 161 (2011).
- [13] K. Dusling, T. Epelbaum, F. Gelis, R. Venugopalan, Phys. Rev. **D 86**, 085040 (2012).
- [14] L.D. McLerran, R. Venugopalan, Phys. Rev. **D 49**, 3352 (1994).
- [15] T. Epelbaum, F. Gelis, Phys. Rev. **D 88**, 085015 (2013).
- [16] G.D. Moore, Nucl. Phys. **B 480**, 689 (1996).
- [17] P. Arnold, G.D. Moore, L. Yaffe, JHEP **0011**, 001 (2000).
- [18] M. Asakawa, S.A. Bass, B. Muller, Phys. Rev. Lett. **96**, 252301 (2006).
- [19] J.P. Blaizot, F. Gelis, J. Liao, L. McLerran, R. Venugopalan, Nucl. Phys. **A 873**, 68 (2012).
- [20] T. Epelbaum, F. Gelis, Nucl. Phys. **A 872**, 210 (2011).
- [21] J.P. Blaizot, J. Liao, L.D. McLerran, arXiv:1305.2119.
- [22] J. Berges, D. Sexty, Phys. Rev. Lett. **108**, 161601 (2012).
- [23] J. Berges, S. Schlichting, D. Sexty, Phys. Rev. **D 86**, 074006 (2012).
- [24] A. Kurkela, G.D. Moore, Phys. Rev. **D 86**, 056008 (2012).
- [25] A. Kurkela, G.D. Moore, JHEP **1111**, 120 (2011).
- [26] A. Kurkela, G.D. Moore, JHEP **1112**, 044 (2011).
- [27] M. Attems, A. Rebhan, M. Strickland, Phys. Rev. **D 87**, 025010 (2013).
- [28] J. Berges, K. Boguslavski, S. Schlichting, Phys. Rev. **D 85**, 076005 (2012).
- [29] J. Berges, S. Schlichting, Phys. Rev. **D 87**, 014026 (2013).
- [30] J. Berges, K. Boguslavski, S. Schlichting, R. Venugopalan, arXiv:1303.5650.